

Article

Not peer-reviewed version

---

# The Collapse of a Neutrino Star Singularity: The Mechanism of the Big Bang?

---

[Jian-Bin Bao](#)<sup>\*</sup> and Nicholas Bao<sup>\*</sup>

Posted Date: 3 January 2024

doi: 10.20944/preprints202401.0136.v1

Keywords: cosmology; cosmic background radiation – early Universe



Preprints.org is a free multidiscipline platform providing preprint service that is dedicated to making early versions of research outputs permanently available and citable. Preprints posted at Preprints.org appear in Web of Science, Crossref, Google Scholar, Scilit, Europe PMC.

Copyright: This is an open access article distributed under the Creative Commons Attribution License which permits unrestricted use, distribution, and reproduction in any medium, provided the original work is properly cited.

Article

# The Collapse of a Neutrino Star Singularity: The Mechanism of the Big Bang?

Jian-Bin Bao <sup>1,2,\*</sup> and Nicholas P. Bao <sup>3,\*</sup><sup>1</sup> Zhejiang University Alumni Association, Hangzhou, Zhejiang 310027, P. R. China<sup>2</sup> University of Alberta Alumni Association, Edmonton, Alberta T5J 4P6, Canada<sup>3</sup> Faculty of Science, University of Alberta, Edmonton, Alberta T6G 2E1, Canada

\* Correspondence: author. Email: jbbao@hotmail.com; nbao@ualberta.ca

**Abstract:** The BKL singularity inside a rotating black hole would be a neutrino star. Once its mass exceeds the limit that neutrino degeneracy pressure could support (larger than  $3 \times 10^{22} M_{\odot}$ ), the neutrino star singularity would collapse, raising the temperature to the maximum and dropping the entropy to the minimum to initiate a Big Bang. From the cosmic microwave background, we find where the Big Bang occurred at about 0.66 times the radius of the surface of last scattering away from us and at Galactic coordinates  $(l, b) \simeq (286^{\circ}, -43^{\circ})$ . As it expands, the clockwise spinning universe has been veering towards the ellipsoidal. These findings are consistent with independent observations of cosmic inhomogeneities, spatial anisotropies, and time variations.

**Keywords:** cosmology; cosmic background radiation — early Universe

## Introduction

According to the sub-extremal Kerr metric in Boyer–Lindquist coordinates, a rotating black hole has two event horizons. Objects in the exterior universe ( $\Delta > 0$ ), by crossing the outer horizon  $r_+$ , can only fall unidirectionally to decrease  $r$ -coordinate ( $\Delta < 0$ ). As the objects enter the inner horizon  $r_-$ , space and time are inversed back ( $\Delta > 0$ ). The maximum analytical extension suggests that the objects could exit from the inner horizon, pass through the unidirectional zone, and enter a new universe. This hypothetical path (Figure 1) is a wormhole, but might not be traversable<sup>1</sup>. Its throat is in the inner horizon with three singularities<sup>2</sup>, at the center of which is a violet, lethal Belinski–Khalatnikov–Lifshitz (BKL) singularity<sup>2–4</sup>. The BKL singularity is also a Weyl singularity<sup>5</sup>, at which the Weyl curvature diverges to infinity:  $C_{abcd} = \infty$ , corresponding to the maximum entropy (Penrose's Weyl curvature hypothesis<sup>4</sup>).

It is believed that the universe started from a pure energy Ricci singularity ( $r = 0$ ), at which the Weyl curvature vanishes:  $C_{abcd} = 0$ , equivalent to the minimum entropy<sup>4</sup>. The mass-energy, including spacetime, of the universe was generated from the Big Bang; the universe was a white hole. This evolution can also be seen in Figure 1.

Now if we divide the whole evolution curve outside the outer horizons, we obtain wormholes. If we divide it inside the inner horizons, we have aeons. Shall we recognize Nature as wormholes or aeons? The latter! As “the endpoint of evolution”<sup>6</sup>, the BKL singularity is a natural watershed to section the evolution curve. Each aeon starts from a Ricci singularity, then develops, and eventually concludes at (multiple) BKL singularities. The Second Law of thermodynamics is valid for individual aeons.

The critical question left unanswered is about the crossover between aeons. As soon as the Weyl singularities were discovered, King predicted the direction of evolution by stating that “the Weyl singularities are unstable against degenerating into ‘big bang’ singularities: should any matter be projected into them it seems certain that we would get  $\rho \rightarrow \infty$ ”<sup>5</sup>. As discussed in Penrose's work<sup>7</sup>, Wheeler, Smolin, and others made the same prediction that “new aeons emerge from black-hole singularities.” Penrose also suspected the origination of “[the Big Bang] singularity from [a] wildly chaotic black-hole riddled (BKL?) collapse,” though he opted to the ultimate hypersurface  $J^+$  for his

conformal cyclic cosmology (CCC)<sup>7</sup>. In this work, we show how the collapse of the BKL singularity initiated the Big Bang.

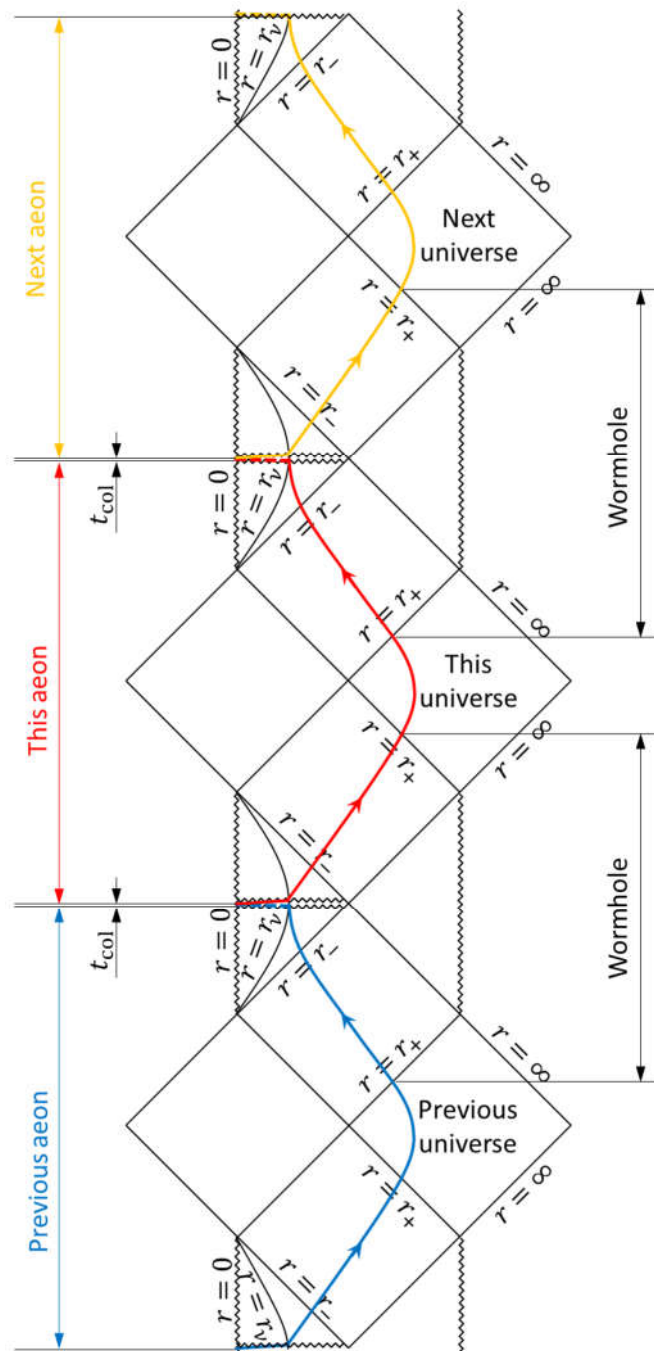


**Figure 1. Penrose diagram of the sub-extremal Kerr spacetime.** The evolution curve is divided into aons (blue, red, and orange). Inside inner horizons  $r_-$ , neutrino stars (future-spacelike BKL singularities) collapse (dash lines,  $t_{col} \sim 10^{-32}$  sec) into timelike Ricci singularities and initiate Big Bangs with spacetimes and neutrino stars (past-spacelike BKL singularities) of new aons. If the evolution curve is divided outside the outer horizons, hypothetical wormholes are obtained.

### Collapse of a Neutrino star Singularity

By studying the fundamental particles and reactions of Nature, we find that the BKL singularity would be a neutrino star. While the detail is in our early work<sup>8</sup>, a brief discussion is provided here. Neutrinos have long been found to be related to vacuum energy<sup>9</sup>. The neutrino mass would be tied up with the energy density of the vacuum by a reversible reaction:

$$A + \bar{A} \rightleftharpoons \gamma + \gamma \quad (1)$$

The fundamental spacetime particles  $A$  and  $\bar{A}$  would annihilate at neutrinos with the release of dark energy into the vacuum, while the energy of the vacuum would recreate the spacetime particles at arbitrary distances (appear as quantum fluctuations). Based on this dynamic equilibrium, estimated from the vacuum energy density<sup>9</sup>:  $\varepsilon_{\text{vac}} \gtrsim \frac{m_{\nu}^4 c^5}{16\pi^2 \hbar^3}$ , the upper limit of the mass of the lightest neutrino:  $m_{\nu} \lesssim 8 \text{ meV}$ .

Neutrinos (larger particles such as neutrons have crushed) would accumulate in the inner horizon, forming a neutrino star (its real geometric shape would not be of importance). More importantly, because spacetime annihilates at neutrinos (the forward of reaction 1), the neutrino star, at which geodesics are terminated, would be a spacetime singularity. The annihilation would inevitably accompany with the recreation of spacetime due to high local energy density (the reverse of reaction 1), so the neutrino star singularity would be very chaotic. The recreated spacetime particles and their energy form would not be immobilized (because they are not neutrinos) at the neutrino star, but thrown out as *emission beams* symmetrically about it (Figure 2). Therefore, spacetime would be stretched along the beams while squashed along the other directions. By approaching the highly compacted, spinning neutrino star, spacetime would become more and more violet and diverge to an infinity curvature. All these characters match those at the BKL singularity<sup>2,4</sup>. Therefore, unlike any observable astronomical object, a neutrino star would be a singularity hidden within a black hole (Penrose's weak cosmic censorship hypothesis).

As neutron degeneracy pressure supports neutron stars, neutrino degeneracy pressure would prevent neutrino stars from collapsing. Analogous to the Tolman-Oppenheimer-Volkoff limit for neutron stars, we estimate a mass limit for neutrino stars:

$$M_{\nu} \approx \left(\frac{m_n}{m_{\nu}}\right)^2 M_n \gtrsim \left(\frac{939.6 \text{ MeV}}{8 \text{ meV}}\right)^2 \times 2.2 M_{\odot} = 3 \times 10^{22} M_{\odot} \quad (2)$$

where  $m_n$ ,  $M_n$ , and  $M_{\odot}$  are the masses of a neutron, a neutron star, and the sun, respectively. Another method to estimate the mass limit is to calculate the Jeans mass of the neutrino<sup>10</sup>:

$$M_{J,\nu} = \frac{1.8 M_{\text{Pl}}^3}{m_{\nu}^2} \gtrsim \frac{1.8 \times (1.22 \times 10^{19} \text{ GeV})^3}{(8 \text{ meV})^2} = 5 \times 10^{22} M_{\odot} \quad (3)$$

where  $M_{\text{Pl}}$  is the Planck mass. Without considering any addition due to the rotation of black holes, both lowermost values estimated from the uppermost neutrino mass are close to the mass of the observable universe, ca.  $10^{23} M_{\odot}$ . Estimated from the smallest neutrino size (the measured cross section<sup>9</sup> is  $10^{-56} \text{ cm}^2$ , identical to the unification distance in the grand unified theory,  $10^{-28} \text{ cm}$ ) the volume of a neutrino star with  $M_{\nu}$  would be as small as  $6 \text{ m}^3$  (equivalent to  $r_{\nu} = 1 \text{ m}$ ).

As King<sup>5</sup> foresaw, matter and energy keep falling into a black hole (not an isolated system), so its mass would eventually exceed  $M_{\nu}$ , resulting in a further collapse. Like any other Oppenheimer-Snyder collapse, it would tremendously raise the temperature (all neutrinos annihilate into pure energy,  $T > T_{\text{Pl}} = 1.4 \times 10^{32} \text{ K}$ ). At such a high temperature, it is natural that the entropy would reach the minimum:  $S \equiv \frac{U-F}{T} < \frac{M_{\nu} c^2}{T_{\text{Pl}}} = 3 \times 10^{60} k_B$ , where  $k_B$  is the Boltzmann constant. In short, as a neutrino star (a future-spacelike singularity,  $r = 1 \text{ m}$ ,  $S \approx \frac{4\pi k_B G M_{\nu}^2}{\hbar c} = 1 \times 10^{122} k_B$ ) collapses into a timelike Ricci singularity ( $r = 0$ ,  $S < 3 \times 10^{60} k_B$ ), a new aeon would start (Figure 1), with expanding spacetime and a new neutrino star (a past-spacelike singularity,  $r = 1 \text{ m}$ ,  $S = 3 \times 10^{60} k_B$ ). This collapse-expansion procedure has been called the *Big Bounce*; the collapse would be a process opposite to the cosmological inflation<sup>11</sup>. Thus the evolution curve (Figure 1) would make very small angles with the horizontal right before and after the Big Bang ( $|dr/dt| \gg c$ ,  $-10^{-32} \text{ sec} \leq t \leq 10^{-32} \text{ sec}$ ), and have a U-turn at the Big Bang ( $t = 0$ ). While the collapse at a specific black hole is an ultrashort ( $\sim 10^{-32} \text{ sec}$ ) entropy fluctuation, the Second Law would still be sustained for the entire evolving system (i.e. Nature, a truly isolated system). As Zel'dovich<sup>6</sup> pointed out, for "cosmological

collapse and black holes," "the general solution of Einstein's equations is highly anisotropic near the [BKL] singularity;" for "cosmological expansion and white holes," "the Kasner solution transform[s] into an isotropic expansion". By studying the *collisions* between the anisotropic spacetime from before the Big Bang and the isotropic expansion after the Big Bang, we would find where the Big Bang occurred or the Center of the universe.

### The Center and Spin of the Universe

The emission beams  $V_b$  (Figure 2) symmetric about the neutrino star, due to weaker collisions with the isotropic Big Bang wave  $V_{BB}$ , result in two cold spots in the cosmic microwave background (CMB, Figure 3A): NC, corresponding to Cold Spot I<sup>12</sup> and Peak 1<sup>13,14</sup>, at  $(l, b) = (318^\circ, -5^\circ)$ , and SC, corresponding to Cold Spot II<sup>12</sup> and Peak 5<sup>13,14</sup>, at  $(l, b) = (208^\circ, -56^\circ)$ . The spiral flows  $V_s$  falling towards the neutrino star (Figure 2), because of stronger collisions with the  $V_{BB}$ , lead to a hot ring. The Center is at the intersection of the  $V_b$  line (line NC-SC) and the  $V_s$  plane determined by the following methods.

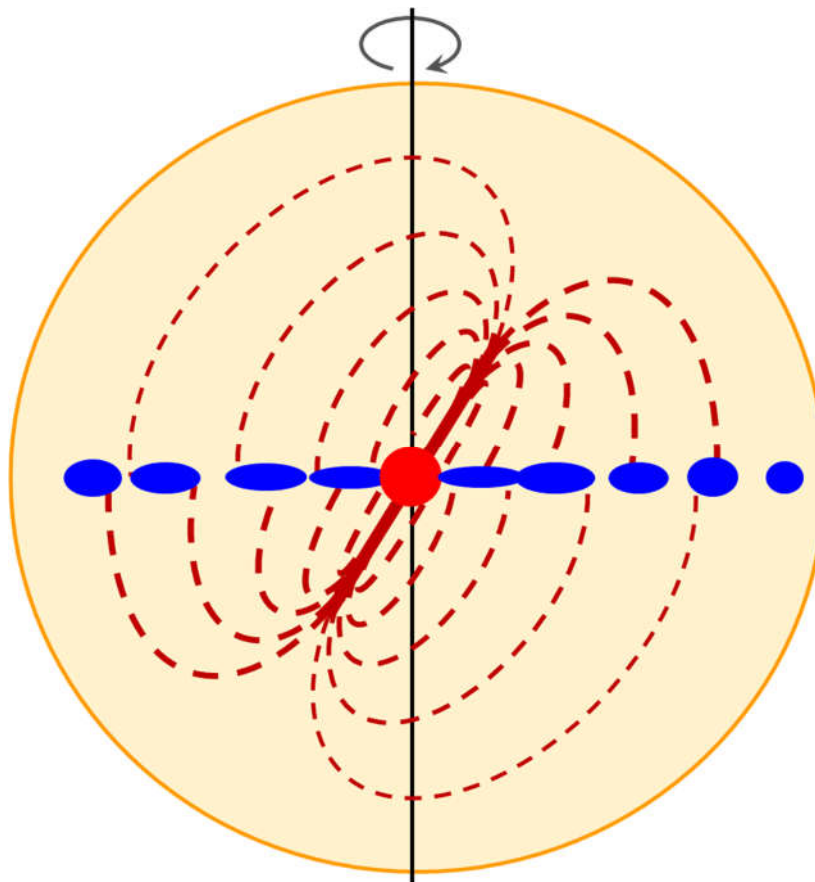


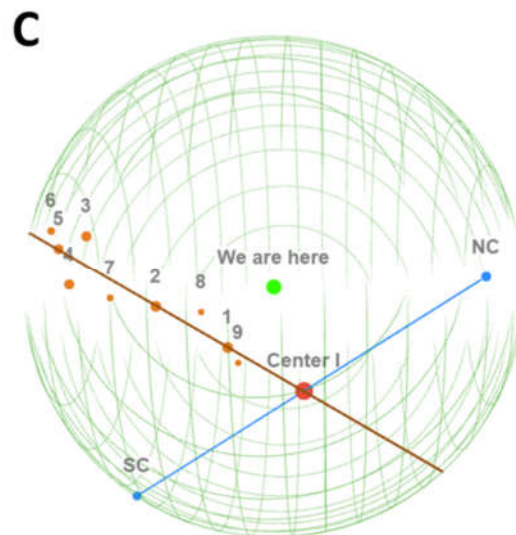
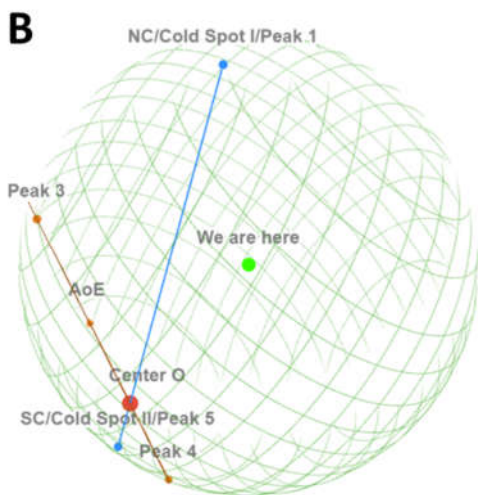
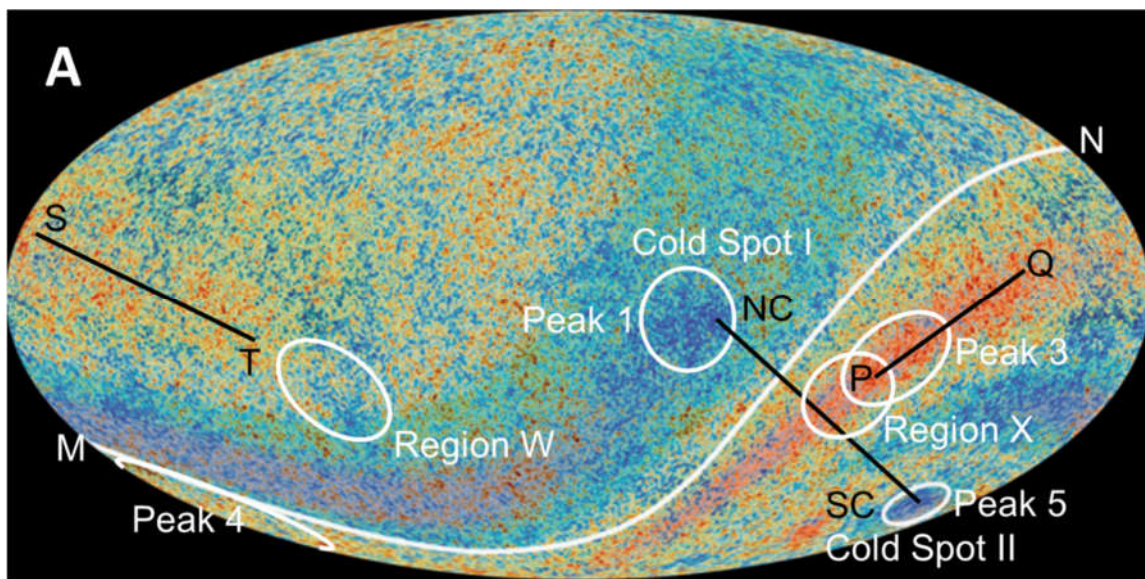
**Figure 2. A schematic diagram of the inner horizon of a rotating black hole.** The eclipse (yellow) is the inner horizon. The eclipse (red) represents a neutrino star. The vertical line (black) is the axis of spin. The horizontal row of clumps (blue) represents the falling spiral flows  $V_s$ , going in on the left and coming out on the right. The slashed lines (dark red) are the emission beams  $V_b$ , developing symmetrically about the neutrino star. The dashed curves (dark red) represent the back falling flows  $V_f$ , either immediately surrounding the  $V_b$  or further into the  $V_s$  plane.

The most noticeable hot region is the large-scale Peak 3 at  $(l, b) = (265^\circ, -20^\circ)$  (from the figures in ref.<sup>14</sup>), which, with Peak 4 at  $(l, b) = (173^\circ, -46^\circ)$ <sup>15</sup>, is known as the Axis of Evil<sup>16,17</sup> (AoE, Figure 3A), whose vector is in the direction  $(l, b) = (250^\circ, 60^\circ)$ <sup>16</sup>. While the AoE offers an interesting starting point, Peak 4 is too close to SC or the  $V_b$  (Figure 3B), and hence would not be from the  $V_s$ ; the calculated intersection (Method O, Table 1) does not seem to match astronomical observations.

**Table 1.** The Center of the universe.

Method	Primary data	Ref	$V_s$ plane	Center ( $l, b$ )	$d/r_{SL}$	$S$
O	Peaks 3, 4 & AoE vector	14-16	$z=-1.54x-1.28y-1.67r_{SLS}$	$(222^\circ, -58^\circ)^a$	0.87	0.1
I	Arcs $PQ, ST$	this work	$z=-0.58x+0.03y-0.36r_{SLS}$	$(286^\circ, -43^\circ)$	0.66	0.5
IIA	Regions $X, W$	21		$(281^\circ, -46^\circ)^b$	0.67	0.4
IIB	Regions $X, W$ & Peak 3	14, 21	$z=-0.74x-0.10y-0.50r_{SLS}$	$(278^\circ, -48^\circ)$	0.67	0.4

a) the preliminary trial that did not pass the synchronous test ( $S$  is far away from 0.5); b) the point on line  $NC$ - $SC$  closest to line  $XW$ .



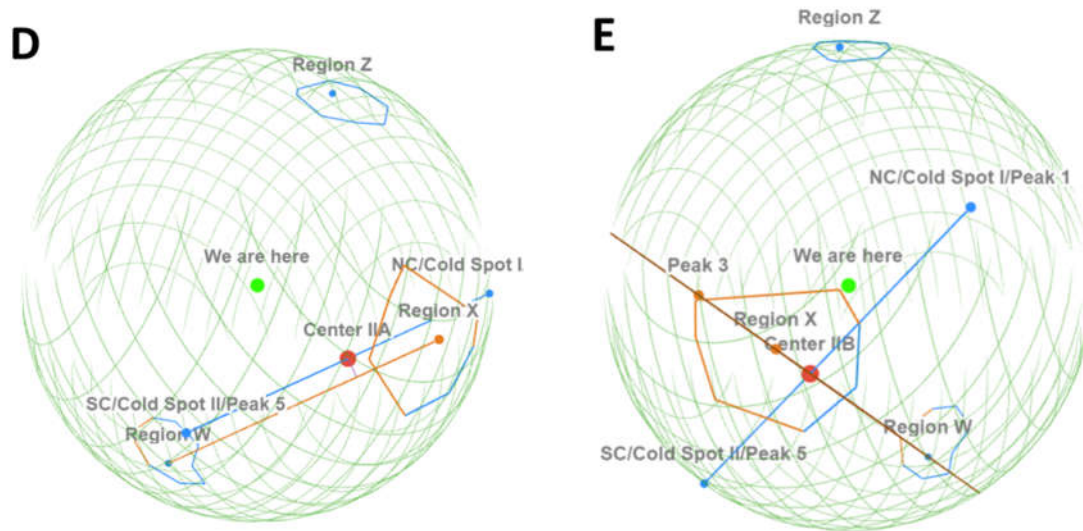


**Figure 3. Methods to determine the Center of the universe.** (A) The Planck CMB map is taken from ref.<sup>17</sup>. All the white symbols and labels are from the literature, and all the blacks from this work. The Center is at the intersection of line NC-SC (the  $V_b$  line) and a hot plane (the  $V_s$  plane): (B) Center O: determined by Peaks 3 and 4, and the AoE ( $MN$ ) vector; (C) Center I: determined by arcs  $PQ$  (1-2-3&4-5) and  $ST$  (6-7-8-9); (D) Center IIA: the closest point on line NC-SC to line  $XW$ ; (E) Center IIB: determined by Regions X and W, and Peak 3. Region X shows a cold corner (blue); region W shows a hot corner (orange). Other symbols are the LS (green) and 3D globe of the SLS (green).

By reanalyzing the CMB, we find that arc  $ST$  (Figure 3A), similar to Peak 3, shows large-scale high temperatures. Thus arcs  $PQ$  and  $ST$  are used to determine the  $V_s$  plane (Figure 3C):

$$z = (-0.58 \pm 0.10)x + (0.03 \pm 0.03)y - (0.36 \pm 0.06)r_{\text{SLS}} \quad (4)$$

where  $r_{\text{SLS}}$  is the radius of the surface of last scattering (SLS). It intersects line NC-SC at  $(l, b) = (286^\circ \pm 10^\circ, -43^\circ \pm 7^\circ)$  and at a distance  $(0.66^{+0.03}_{-0.01})r_{\text{SLS}}$  away from where we are (hereafter represented by the Local Supercluster or LS) (Method I, Table 1). Since  $r_{\text{SLS}} = 14 \text{ Gpc}$ <sup>18</sup>, the Center is ca. 9.3 Gpc or 30 billion light years away from us. Only half of the hot ring (arcs  $PQ$  and  $ST$ ) is observed, while the other half is hardly visible. This is due to the Doppler effect and the Doppler beaming: the  $V_s$  flows were spiraling towards the precursor neutrino star (Figure 2). We therefore find that: i) if we look from the LS to the Center, the universe is rotating or spinning clockwise; ii) the  $V_s$  plane is the equatorial plane of the universe; iii) the LS is inside the Northern observable universe; iv) the Northern observable universe is bigger than the Southern; v) the axis of spin of the universe is:

$$(x, y, z) = (0.13r_{\text{SLS}}, -0.47r_{\text{SLS}}, -0.45r_{\text{SLS}}) + (0.58, -0.03, 1.00)t \quad (5)$$

vi) the spin axis intersects with the SLS at  $(l, b) = (325^\circ, 31^\circ)$  and  $(256^\circ, -62^\circ)$ ; vii) the angle between the equatorial plane and the Galactic plane is  $30^\circ \pm 5^\circ$ .

Method II is based on the low-variance circles (LVC) that Gurzadyan and Penrose<sup>19,20</sup> found. Regions X and W show characteristic properties of the  $V_s$  flows (Figures 3D and 3E), and therefore are employed to define the  $V_s$  plane. Based on Bodnia *et al.*'s coordinates<sup>21</sup>: Region X at  $(l, b) = (280.1^\circ, -31.5^\circ)$  and Region W at  $(l, b) = (86.1^\circ, -38.2^\circ)$ , line  $XW$  almost intersects line NC-SC (Fig. 3D), so the closest point at  $(l, b) = (281^\circ, -46^\circ)$  and at a distance  $0.67r_{\text{SLS}}$  can be regarded as the Center (Method IIA, Table 1). If the Regions are used to define the  $V_s$  plane with Peak 3 (Figure 3E), then the Center is at  $(l, b) = (278^\circ, -48^\circ)$  and at a distance  $0.67r_{\text{SLS}}$  (Method IIB, Table 1). These results are virtually the same as those from Method I.

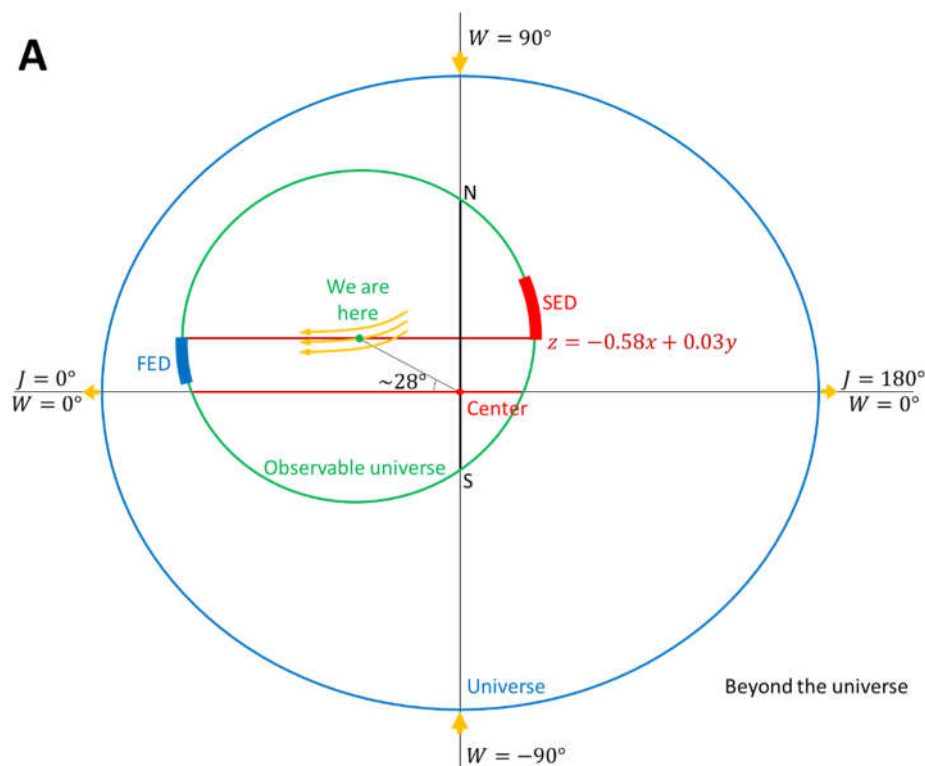
### Paradox of the Existence of the Center

It is generally believed that the universe has no center, with the reason being that the Big Bang happened everywhere, or that the Hubble flow is observed everywhere. Another would argue that it is nonsense to locate a center within the universe, as space itself was from the Big Bang. Based on our mechanism, the universe is finite and has a center. As in the raisin bread model, the center of the bread is the dough before baking (without gravity), the Center is where the precursor black hole collapsed in the previous aeon and now in the present aeon.

One might also wonder how our mechanism could generate an isotropic and homogeneous universe. It is important to first note that more and more astronomical observations have shown that the universe has small magnitudes of anisotropies and inhomogeneities (details below). Based on our mechanism, any potential massive objects near the precursor neutrino star would have been merged. Without the influence of the surroundings (all the flows discussed above were negligible), the newborn universe was isotropic and homogeneous<sup>4,6</sup>. During the course of expansion, Hubble's law is always valid, even for objects with separation greater than the Hubble length<sup>22,23</sup>. An analysis of the CMB indicates that anisotropic expansion is strongly disfavoured, with odds of 121,000:1 against<sup>24</sup>. The only deviation away from the cosmological principle is from the centrifugal force that has been deforming the universe. Therefore, while the local universe looks almost isotropic and homogeneous, the original uniformity is maintained for an early image such as the CMB, because the deviation due to the spin is dipolar and overshadowed by the peculiar motion. Unless we were near its edge (we are not), the universe from our mechanism appears very isotropic and homogeneous.

### Independent Observational Evidence

While the theoretical analysis indicates that black holes are the embryos of the universes of the next aeons, the match of the results from Methods I and II is a solid piece of direct evidence of our mechanism. Besides them, various independent observational evidence has been reported in the literature. For future convenience, we define a *Universal Coordinate System* (Figure 4A), in which the LS is set at zero degrees longitude and the  $r_{\text{SLS}}$  the unit length. The angle between the line from the Center to the LS and the equatorial plane is ca.  $28^\circ$  and the distance between the LS and the Center is ca.  $0.66r_{\text{SLS}}$ , so the universal coordinates for the LS are:  $(J, W, R) = (0^\circ, +28^\circ, 0.66)$ .





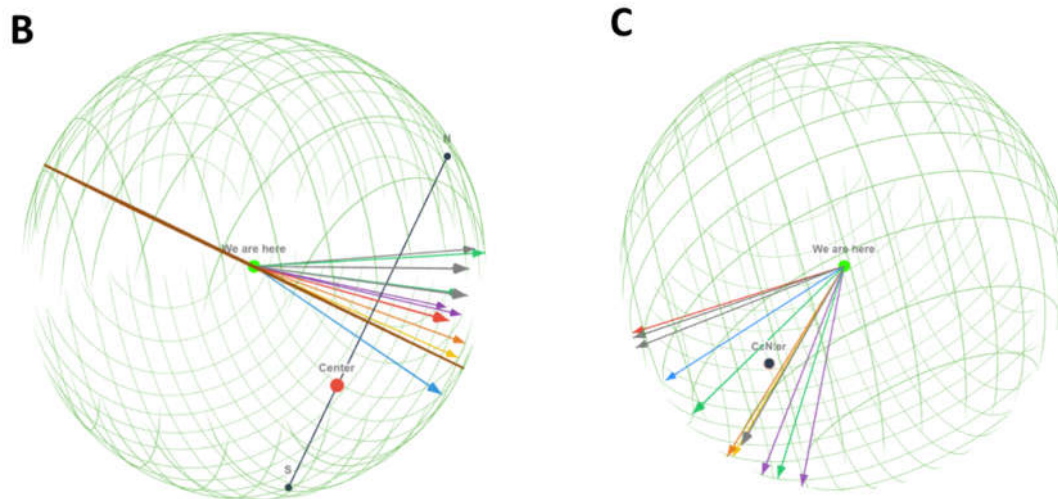


**Figure 4. Anisotropic universe.** (A) A schematic picture for the universe. The universe was born from the Center (red dot) due to the collapse of a neutrino star in Nature. Because the precursor neutrino star span, the universe is ellipsoidal (represented by a blue ellipse), elongated (orange thick horizontal arrow) in the directions parallel to its equator ( $W = 0^\circ$ ) and contracted (orange thick vertical arrow) in the direction parallel to its axis of spin ( $W = \pm 90^\circ$ ). Note that this figure is not to scale, in particular, the size and eccentricity of the universe are unknown. The LS (green dot) is rotating about the axis of spin on the plane (dark red):  $z = -0.58x + 0.03y$ , and moving towards the furthest equatorial plane (the direction of orange thin arrows). The faster expansion: FED (blue direction), and the slower expansion: SED (red direction). The observable universe is nearly ellipsoidal (represented by a green ellipse), within which are: the equatorial plane (red line), and the axis of spin (black line, between N and S). (B) Side view, parallel to the equatorial plane; (C) Top view, along the axis of spin. Unit vectors of the observed SED: CMB dipole (red), galaxy cluster anisotropy (blue), bulk flows (grey), Great Attractor (green), SNe Ia dipole (yellow), dark energy dipole (orange), fine-structure constant dipole (violet). The line (dark red) is the rotational plane of the LS (green). All vectors are plotted in length of the radius of SLS; the other symbols are the same as in Figure 3.

The first category of evidence is the inhomogeneous compositions of the universe. In the inner horizon of the precursor black hole, the  $\mathbf{V}_b$  and  $\mathbf{V}_f$  would sweep in a high angular speed, producing discontinuous clumps of high-density mass-energy across the space (Figure 2). After the Big Bang, these flows, together with the  $\mathbf{V}_s$ , would collide with the  $\mathbf{V}_{BB}$ , resulting in overdense clumps and debris as primordial nucleation centers (PNC) for the formation of primordial black holes or primordial galaxies. In addition to the LVC, some PNC would have been observed as the Hawking points<sup>25</sup>. Compared to structure formation theories in which overdensities are the consequence of minute quantum fluctuations, our mechanism generates the PNC much earlier and more mature, and hence explains multiple extraordinary astronomical facts, such as an unexpectedly large number<sup>26</sup> of unexpectedly mature<sup>26</sup> and unexpectedly bright<sup>27</sup> galaxies observed by the JWST with unexpectedly high mass<sup>28,29</sup> formed at an unexpectedly short time<sup>26</sup>, as well as the extraordinarily large cosmic structures (such as Ho'oleilana<sup>30</sup>) and black holes (candidates<sup>31</sup>: Phoenix A and 4C+74.13, etc.). Note that the first galaxies in the early JWST deep fields<sup>32</sup>, such as SMACS-0723 (close to the Center,  $W \sim +43^\circ$ ), CEERS ( $W \sim +37^\circ$ ), and GLASS ( $W \sim -27^\circ$ ), are in the higher-density zones ( $|W| \leq 58^\circ \pm 6^\circ$ , the angle between line NC-SC and the  $\mathbf{V}_s$  plane), so are the large cosmic structures and black holes<sup>30,31</sup>.

The second category of evidence is cosmic anisotropies. Our mechanism does not provide any massive structures at the Center after the Big Bang (for comparison, before the Big Bang there was a massive neutrino star). With the centripetal force requirement, the spinning universe has been expanding faster along the rotationally radial direction and slower along the axis of spin. Thus the universe has been veering towards the ellipsoidal (Figure 4A). This deformation changes our observable universe accordingly. Campanelli *et al.* suspected that the SLS was ellipsoidal<sup>33</sup>. Strictly

speaking, the observable universe is not ellipsoidal, because it does not have orthogonal axes as the universe does or, equivalently, the LS is not on the equatorial plane. Therefore, the exact direction of the fastest or slowest expansion is unknown, because it is related to the size of the universe that is unknown (the lowermost would be  $3.32r_{\text{SLS}}$ ). If the dominating Hubble flow were removed, while always in the Northern universe, the LS would move *closer* to the equatorial plane. Therefore, the fastest expansion direction (FED) of the observable universe shall be close to the outward rotationally radial direction, skewing towards the equatorial plane (Figure 4A). As the expansion is slower along the axis of spin, the slowest expansion direction (SED) shall be close to the inward rotationally radial direction  $(l, b) = (301^\circ, -18^\circ)$ , skewing away from the equatorial plane (Figure 4A).

This preferred direction is confirmed by multiple independent astronomical observations<sup>34-44</sup>. Probably because the magnitudes of those anisotropies are very small ( $10^{-5} \sim 10^{-3}$ ), the observed directions are scattering for different properties, as well as for the same properties (Figure 4B and 4C). With such small anisotropies, the obtained coordinates of the Center (Table 1), though would bias the North, are unnecessary to correct; the SLS can be regarded as a sphere. Other than the fine-structure constant  $\alpha$  dipole<sup>34,35</sup> that is generally attributed to a different mechanism<sup>45,46</sup>, slower expansion in the SED appears as lower accelerating expansion (dark energy dipole<sup>35</sup>), brighter Type Ia supernovae (SNe Ia dipole<sup>36</sup>), smaller Hubble constant  $H_0$  (galaxy cluster anisotropy<sup>37</sup>), or mutually approaching flows of galaxies (such as bulk flows<sup>38-41</sup>). With the understanding that those anisotropies share the same mechanism, we can convert from one to another.

The third category of evidence is time variations. While the LS is moving away from the direction of the slower expansion (Figure 4A), the universe has been expanding in acceleration<sup>47,48</sup>. While the LS moves away from the direction of the smaller  $H_0$ , the Hubble tension indicates that the  $H_0$  was smaller in the past<sup>49</sup>. While the LS moves away from the direction of the slower expansion or higher matter density and amplitude of growth of structures, the  $S_8$  tension indicates that the  $S_8$  value was larger in the past<sup>50</sup>.

**Data Availability Statement:** All results in this work are obtained using publicly available data.

**Acknowledgments:** J.B.B. would like to thank Profs. Z. Shen, K. Yao, X. Jiang, F. Bo, Y. Cheng, S. Han, G. Chen, and Q. Yu at Zhejiang University for their inspiration. N.P.B. would like to dedicate this work to his grandparents in China.

**Competing Interests:** The authors declare no competing interests.

## References

1. Morris, M. S. & Thorne, K. S. Wormholes in spacetime and their use for interstellar travel: a tool for teaching general relativity. *Am. J. Phys.* **56**, 395-412 (1988).
2. Scheel, M. A. & Thorne, K. S. Geometrodynamics: the nonlinear dynamics of curved spacetime. *Physics-Uspokhi* **57**, 342-351 (2014).
3. Belinskii, V.A., Khalatnikov, I. M. & Lifshitz, E.M. Oscillatory approach to a singular point in the relativistic cosmology. *Adv. Phys.* **19**, 525-573 (1970).
4. Penrose, R. Singularities and Time-Asymmetry. In Hawking, S. W. & Israel, W. (eds) *General Relativity: An Einstein Centenary Survey* (Cambridge University Press, Cambridge, 581-638, 1979).
5. King, A. R. New types of singularity in general relativity: the general cylindrically symmetric stationary dust solution. *Commun. Math. Phys.* **38**, 157-171 (1974).
6. Zel'dovich, Ya. B. Creation of particles in cosmology. In Longair, M. S. (ed) *Confrontation of cosmological theories with observational data* (D. Reidel Pub., Dordrecht, 329-333, 1974).
7. Penrose, R. *Cycles of time: an extraordinary new view of the universe* (Bodley Head, London, 2010).
8. Bao, J. B., Bao, N. P. On the Fundamental Particles and Reactions of Nature. *Preprints* **2020**, 2020120703.
9. Perkins, D. *Particle Astrophysics*. 2nd ed. (Oxford Univ. Press, New York, 2003).
10. Prakash, N. *Dark matter, neutrinos, and our solar system* (World Sci., Singapore, 2013).

11. Guth, A. H. Inflationary universe: a possible solution to the horizon and flatness problems. *Phys. Rev. D* **23**, 347-356 (1981).
12. Bennett, C. L. et al. Seven-year Wilkinson Microwave Anisotropy Probe (WMAP) observations: are there cosmic microwave background anomalies? *Astrophys. J. Supp. Ser.* **192**, 17 (2001).
13. Planck Collaboration: Akrami, Y. et al. Planck 2018 results. VII. Isotropy and Statistics of the CMB. *Astron. Astrophys.* **641**, A7 (2020).
14. Caballero, A. M. The Cosmic Microwave Background radiation at large scales and the peak theory. Univ. Cantabria Thesis (2017).
15. Pietrobon, D. et al. Needlet detection of features in the WMAP CMB sky and the impact on anisotropies and hemispherical asymmetries. *Phys. Rev. D* **78**, 103504 (2008).
16. de Oliveira-Costa, A. et al. Significance of the largest scale CMB fluctuations in WMAP. *Phys. Rev. D* **69**, 063516 (2004).
17. Wright, A. Across the universe. *Nat. Phys.* **9**, 264 (2013).
18. Gott III, J. R. et al. A map of the universe. *Astrophys. J.* **624**, 463-484 (2005).
19. Gurzadyan, V. G. & Penrose, R. On CCC-predicted concentric low-variance circles in the CMB sky. *Eur. Phys. J. Plus.* **128**, 22 (2013).
20. Gurzadyan, V. G. & Penrose, R. CCC and the Fermi paradox. *Eur. Phys. J. Plus.* **131**, 11 (2016).
21. Bodnia, E. et al. Conformal cyclic cosmology signatures and anomalies of the CMB sky. arXiv: 2208.06021v2 (2023).
22. Peebles, P. J. E. *Principles of Physical Cosmology* (Princeton Univ. Press, Princeton, 1993).
23. Davis, T. M. & Lineweaver, C. H. Expanding confusion: common misconceptions of cosmological horizons and the superluminal expansion of the universe. *Pubs. Astr. Soc. Australia* **21**, 97-109 (2004).
24. Saadeh, D. et al. How isotropic is the universe? *Phys. Rev. Lett.* **117**, 131302 (2016).
25. An, D. et al. Apparent evidence for Hawking points in the CMB Sky. *Mon. Not. R. Astron. Soc.* **495**, 3403-3408 (2020).
26. Witze, A. Four revelations from the Webb telescope about distant galaxies. *Nature* **608**, 18-19 (2022).
27. Clery, D. Earliest galaxies found by JWST confound theory. *Science* **379**, 1280-1281 (2023).
28. Labbé, I. et al. A population of red candidate massive galaxies ~600 Myr after the Big Bang. *Nature* **616**, 266-269 (2023).
29. Boylan-Kolchin, M. Stress testing  $\Lambda$ CDM with high-redshift galaxy candidates. *Nat. Astron.* **7**, 731-735 (2023).
30. Tully, R. B., Howlett, C. & Pomarède, D. Ho'oleilana: An individual baryon acoustic oscillation? *Astrophys. J.* **954**, 169 (2023).
31. List of most massive black holes. [https://www.wikipedia.org/wiki/List\\_of\\_most\\_massive\\_black\\_holes](https://www.wikipedia.org/wiki/List_of_most_massive_black_holes).
32. Donnan, C. T. et al. The evolution of the galaxy UV luminosity function at redshifts  $z \simeq 8 - 15$  from deep JWST and ground-based near-infrared imaging. *Mon. Not. R. Astron. Soc.* **518**, 6011-6040 (2023).
33. Campanelli, L., Cea, P. & Tedesco, L. Ellipsoidal universe can solve the CMB quadrupole problem. *Phys. Rev. Lett.* **97**, 131302 (2006).
34. King, J. A. et al. Spatial variation in the fine-structure constant – new results from VLT/UVES. *Mon. Not. R. Astron. Soc.* **422**, 3370-3414 (2012).
35. Mariano, A. & Perivolaropoulos, L. Is there correlation between fine structure and dark energy cosmic dipoles? *Phys. Rev. D* **86**, 083517 (2012).
36. Chang, Z. & Lin, H.-N. Comparison between hemisphere comparison method and dipole-fitting method in tracing the anisotropic expansion of the Universe use the Union2 data set. *Mon. Not. R. Astron. Soc.* **446**, 2952-2958 (2015).
37. Migkas, K. et al. Cosmological implications of the anisotropy of ten galaxy cluster scaling relations. *Astro. Astrophys.* **649**, A151 (2021).
38. Hudson, M. J. et al. A large-scale bulk flow of galaxy clusters. *Astrophys. J.* **512**, L79 (1999).

39. Kashlinsky, A. et al. A measurement of large-scale peculiar velocities of clusters of galaxies: technical details. *Astrophys. J.* **691**, 1479–1493 (2009).
40. Feldman, H. A., Watkins, R. & Hudson, M. J. Cosmic flows on 100 h<sup>-1</sup> Mpc scales: standardized minimum variance bulk flow, shear and octupole moments. *Mon. Not. R. Astron. Soc.* **407**, 2328–2338 (2010).
41. Turnbull, S. J. et al. Cosmic flows in the nearby universe from Type Ia supernovae. *Mon. Not. R. Astron. Soc.* **420**, 447–454 (2012).
42. Abdalla, E. et al. Cosmology intertwined: A review of the particle physics, astrophysics, and cosmology associated with the cosmological tensions and anomalies. *J. High Energy Astrophys.* **34**, 49–211 (2022).
43. Perivolaropoulos, L. & Skara, F. Challenges for  $\Lambda$ CDM: An update. *New Astron. Rev.* **95**, 101659 (2022).
44. Aluri, P. K. et al. Is the Observable Universe Consistent with the Cosmological Principle? *Class. Quantum Grav.* **40**, 094001 (2023).
45. Davies, P. C. W., Davis, T. M. & Lineweaver, C. H., Black holes constrain varying constants. *Nature* **418**, 602–603 (2003).
46. Carlip, S. & Vaidya, S. Do black holes constrain varying constants? *Nature* **421**, 498 (2003).
47. Perlmutter, S. et al. Measurement of  $\Omega$  and  $\Lambda$  from 42 high-redshift supernovae. *Astrophys. J.* **517**, 565–586 (1999).
48. Riess, A. G. et al. Observational evidence from supernovae for an accelerating universe and a cosmological constant. *Astron. J.* **116**, 1009–1038 (1998).
49. Riess, A. G. et al. A comprehensive measurement of the local value of the Hubble constant with 1 km/s/Mpc uncertainty from the Hubble Space Telescope and the SH0ES team. *Astrophys. J. Lett.* **934**, L7 (2022).
50. Battye, R. A., Charnock, T. & Moss, A. Tension between the power spectrum of density perturbations measured on large and small scales. *Phys. Rev. D* **91**, 103508 (2015).

**Disclaimer/Publisher's Note:** The statements, opinions and data contained in all publications are solely those of the individual author(s) and contributor(s) and not of MDPI and/or the editor(s). MDPI and/or the editor(s) disclaim responsibility for any injury to people or property resulting from any ideas, methods, instructions or products referred to in the content.